

Supporting information for

**A Star-Shaped Molecule with Low-Lying Lowest Unoccupied
Molecular Orbital Level, n-type Panchromatic Electrochromism, and
Long-Term Stability**

Bin Yao, Yue Zhou, Xichong Ye, Rong Wang, Jie Zhang* and Xinhua Wan*

Beijing National Laboratory for Molecular Sciences, Key Laboratory of Polymer Chemistry and Physics of Ministry of Education, College of Chemistry and Molecular Engineering, Peking University, Beijing 100871, China

*E-mail: xhwan@pku.edu.cn (Xinhua Wan); jz10@pku.edu.cn (Jie Zhang).

Part 1. General Information	S1–S2
Part 2. Experimental Procedures	S3–S6
Part 3. TGA, DPV, Absorptions, EPR, and Electrochromic Data	S7–S9
Part 4. XRD, DSC, POM, 1D-WAXD, 1D-WAXD	S10–S12
Part 5. ¹ H NMR and ¹³ C NMR Spectra	S13–S17

Part 1. General Information

All reagents were obtained from J&K, Aldrich, Acros, and TCI Chemical Co., and used as received unless otherwise specified. CH₂Cl₂ and CH₃CN were purified by distillation over CaH₂. ¹H NMR spectra and ¹³C NMR spectra were measured on a Bruker ARX400 spectrometer (400 MHz) at the ambient temperature with CDCl₃ as the solvent and tetramethylsilane (TMS) as an internal standard. Chemical shifts were reported in ppm with TMS (0 ppm) as standard. High-resolution mass spectra were recorded on a Bruker APEXIV Fourier transform ion cyclotron resonance mass spectrometer. MALDI-TOF mass spectra were recorded on an ABI 4800 Plus MALDI TOF/TOF™ Analyzer.

UV–vis absorption spectra of the compounds were recorded on a Hitachi U-4100 spectrophotometer using 1-mm quartz cell. Thermogravimetric analyses (TGA) were performed on a TA Instrument Q600 analyzer under different gas a flow rate of 100 mL min⁻¹. DSC measurements were performed on a TA Q100DSC analyzer under nitrogen with a heating rate of 20 °C /min and cooling rate of 2 °C /min.

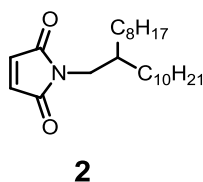
Cyclic voltammetry and differential pulse voltammetry were carried out on a CHI840B electrochemical workstation. The solutions were made in CH₂Cl₂ (5 × 10⁻⁴ mol/L) containing 0.1 M tetra-n-butylammonium hexafluorophosphate (TBAPF₆) as an electrolyte and were degassed with nitrogen prior to electrochemical work. Platinum working and counter electrodes were employed together with a silver pseudoreference electrode. The pseudo-reference was calibrated externally using a solution of ferrocene (Fc/Fc⁺). The scanning direction was negative since the reduction potentials were more concerned. Spectroelectrochemical data were performed on a Hitachi U-4100 spectrophotometer connected to a computer in an optical transparent thin layer (OTTLE) cell or through the thin film on ITO glass dipped into CH₃CN/TBAPF₆ (0.1M) solution. The solvents CH₂Cl₂ and CH₃CN were distilled over CaH₂ prior to use. The ESR spectrum was recorded on a Bruker ESP-E500 spectrometer. For EPR experiment, the solution was sealed in glass capillary for measurement after reduction to radical anion state.

One-dimensional wide-angle X-ray diffraction (1D WAXD) experiments were run on a Philips X'Pert Pro diffractometer with a 3 kW ceramic tube as the X-ray source (Cu Ka) and an X'celerator detector. The sample stage was set horizontally. The reflection peak positions were calibrated against silicon powder (2q > 15°) and silver behenate (2q < 10°). Background scattering was recorded and subtracted from the sample patterns. Two-dimensional wide-angle X-ray diffraction (2D WAXD) experiments were performed on a Bruker D8 Discover diffractometer. The sample was oriented at 200 °C and then quenched to room temperature.

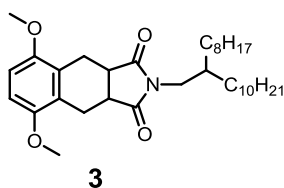
The geometry of the molecules was optimized with density functional theory (DFT) using B3LYP hybrid functional with a basis set limited to 6-31g+G(d). Each optimization was verified by frequency analysis for real energy minimization.

Molecular orbital shapes were performed at optimized geometries with theory level at B3LYP/6-31+G(d). Quantum-chemical calculation was performed with the Gaussian09 package¹ and the orbital pictures were prepared using Gaussview². To simplify the calculations, the substituent on imide was simplified as a methyl group.

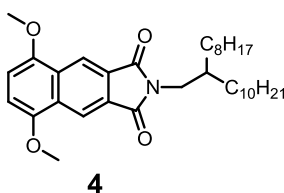
Part 2. Experimental Procedures



Maleic anhydride (0.98 g, 10 mmol), 2-octyldodecyl amine (3.13 g, 10.5 mmol), and 20 mL benzene was added into a three-neck flask under N₂. The solution was stirred for 1 h at 30 °C, and then ZnBr₂ (2.25 g, 10.0 mmol) and hexamethyl disilazane (2.20 g, 13.6 mmol) were added. The resultant suspension was heated to reflux for another 2 hour. After cooling to room temperature, the mixture was poured into 60 mL of 0.5 M aqueous HCl and extracted with 3 × 40 mL CH₃COOEt. The combined organic phase was washed with saturated NaHCO₃ solution several times and then washed with saturated NaCl once, dried with Na₂SO₄, and filtered, and the solvent was removed under reduced pressure. The crude product was purified by silica gel chromatography (CH₂Cl₂/petroleum ether = 1/1 (v/v) as eluent, *R_f* = 0.60) to afford a colorless transparent liquid (3.16 g) in 84% yield. ¹H NMR (400 MHz, CDCl₃): δ 6.68 (s, 1H), 3.40 (d, *J* = 7.2 Hz, 2H) 1.76 (m, 1H), 1.32–1.20 (m, 32H), 0.88(t, *J* = 6.8 Hz, 6H). ¹³C NMR (100 MHz, CDCl₃): δ 171.15, 133.96, 42.15, 36.96, 31.93, 31.90, 31.40, 29.98, 29.65, 29.64, 29.59, 29.54, 29.35, 29.30, 26.25, 22.69, 22.68, 14.12. ESI-HRMS [M+H]⁺: 378.33578, C₂₄H₄₄NO₂ requires 378.33666.

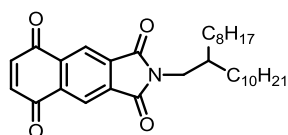


1,4-dimethoxy-2,3-bis(bromomethyl)benzene³ (1.30 g, 4.00 mmol), compound **2** (1.59 g, 4.10 mmol), NaI (3.00 g, 20.0 mmol), and DMF (25 mL) were successively added to a 100 mL three-neck flask under N₂. The mixture turned a brown/black color during the reaction system was heated to 90 °C and was stirred for 48 h at 90 °C under N₂. After cooling to room temperature, the mixture were poured into 100 mL water and extracted with 3 × 50 mL CH₂Cl₂. The combined organic phase was washed with 3 × 150 mL 0.5 M NaHSO₃ aqueous solution, 3 × 150 mL dilute HCl aqueous solution and then 200 mL saturated NaCl once, dried with Na₂SO₄, and filtered, and the solvent was removed under reduced pressure. The crude product was purified by silica gel chromatography (CH₂Cl₂ as eluent, *R_f* = 0.40) to afford a light yellow oily liquid (1.14 g) in 53% yield. ¹H NMR (400 MHz, CDCl₃): δ 6.67 (s, 1H), 3.74 (s, 6H), 3.56–3.48 (m, 2H), 3.26–3.18 (m, 4H), 3.64–3.56 (m, 2H), 1.46 (m, 1H), 1.32–1.04 (m, 28H), 0.92–0.72 (m, 10H). ¹³C NMR (100 MHz, CDCl₃): δ 179.85, 150.75, 125.20, 109.75, 56.44, 42.73, 39.42, 35.99, 31.93, 30.68, 29.90, 29.70, 29.67, 29.66, 29.37, 29.35, 25.99, 22.69, 21.80, 14.12. ESI-HRMS [M+H]⁺: 542.42156, C₃₄H₅₆NO₄ requires 542.42039.



0.45 g TsOH·H₂O and 60 mL toluene were added to a 150 mL three-neck flask which equipped a manifold. The mixture were heated to reflux for 3 h to remove the crystal water in TsOH·H₂O. After cooling to room temperature, compound **3** (1.14 g, 2.10 mmol) and 2,3-dichloro-5,6-dicyanobenzoquinone (DDQ, 1.69 g, 7.50 mmol) were added to the flask, respectively. The solution turned red/black immediately when DDQ was added and was heated to reflux for another 24 h. After cooling to room temperature, the solution was filtrated and washed three times with toluene. Toluene

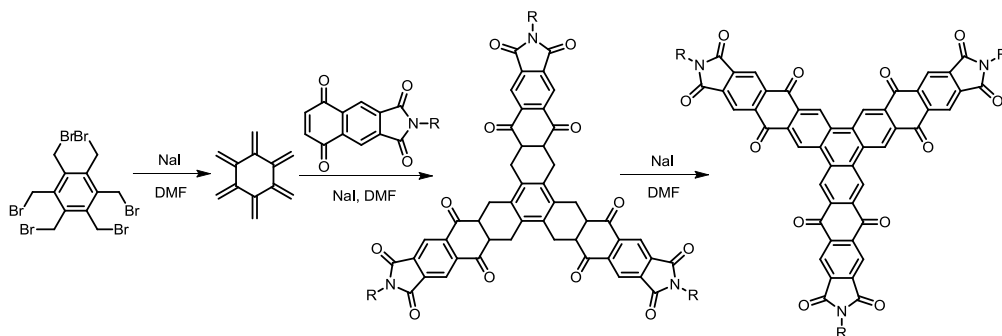
was removed under reduced pressure, and 100 mL CH₂Cl₂ was added to dissolve the residue. The organic solution was washed with 3 × 100 mL saturated NaHCO₃ and 150 mL saturated NaCl once, dried with Na₂SO₄, and filtered, and the solvent was removed under reduced pressure. The crude product was purified by silica gel chromatography (CH₂Cl₂/petroleum ether = 4/3(v/v) as eluent, *R_f* = 0.50) to afford a yellow waxy solid (0.46 g) in 40% yield. ¹H NMR (400 MHz, CDCl₃): δ 8.72 (s, 2H), 6.91 (s, 2H), 3.99 (s, 6H), 3.63 (d, *J* = 7.2 Hz), 1.94 (m, 1H), 1.40–1.18 (m, 32H), 0.89–0.83 (m, 6H). ¹³C NMR (100 MHz, CDCl₃): δ 168.64, 150.95, 128.19, 127.60, 119.11, 107.18, 56.02, 42.57, 36.95, 31.92, 31.90, 31.58, 29.98, 29.63, 29.58, 29.55, 29.34, 29.30, 26.33, 22.68, 14.11, 14.09. ESI-HRMS [M+H]⁺: 538.38998, C₃₄H₅₂NO₄ requires 538.38909.



5

Compound **4** (0.50 g, 0.93 mmol) and 180 mL CH₃CN were added to a 250 mL round bottom flask, and the mixture were stirred for 2 h to form a homogeneous solution at 30 °C. Ceric ammonium nitrate (CAN, 1.27 g, 2.30 mmol) dissolved in 16 mL CH₃CN-H₂O (v/v=1/1) was added dropwise into the solution during 15 minutes, and stirring was continued for 2 h until the compound **4** was consumed which detected by TLC analysis. After most solvent was removed under reduced pressure, 100 mL CH₂Cl₂ was added to dissolve the remaining solid. The organic solution was washed with 3 × 100 mL saturated NaCl, dried with Na₂SO₄, and filtered, and the solvent was removed under reduced pressure. The crude product was purified by silica gel chromatography (CH₂Cl₂ as eluent, *R_f* = 0.55) to afford a yellow solid (0.40 g) in 85% yield. ¹H NMR (400 MHz, CDCl₃): δ 8.57 (s, 2H), 7.14 (s, 2H), 3.64 (d, *J* = 7.2 Hz, 2H), 1.90 (m, 1H), 1.38–1.22 (m, 32H), 0.90–0.84 (tt, 6H). ¹³C NMR (100 MHz, CDCl₃): δ 183.24, 166.69, 138.91, 136.29, 135.80, 121.71, 43.00, 36.97, 31.92, 31.88, 31.49, 29.93, 29.62, 29.57, 29.52, 29.34, 29.28, 26.25, 22.68, 22.67, 14.11. ESI-HRMS [M+H]⁺: 508.34154, C₃₂H₄₆NO₄ requires 508.34214.

Part 3. TGA, DPV, Absorptions, EPR, and Electrochromic Data



Scheme S1. Detailed reaction processes in the last D-A reaction in the synthesis of **6**.

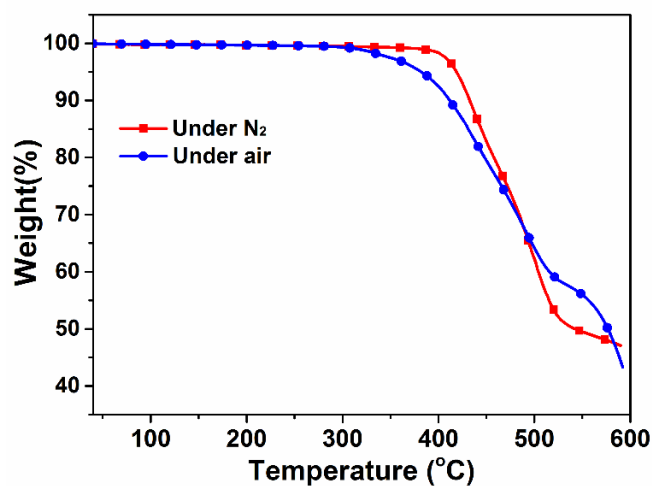


Figure S1. TGA curves of **6** under N₂ (red line) and air (blue line).

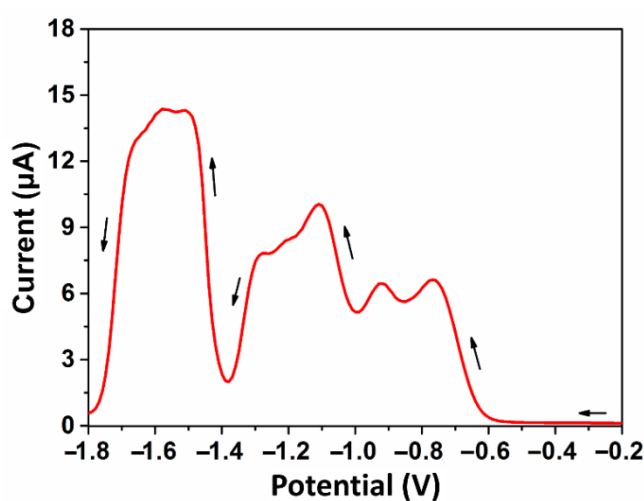


Figure S2. DPV of **6** in CH₂Cl₂ solution at ambient temperature, $c = 5 \times 10^{-4}$ mol/L, 0.1 M TBAPF₆ as an electrolyte, potentials vs Fc/Fc⁺. The black arrows indicate the scanning directions, and the starting point was the less negative side.

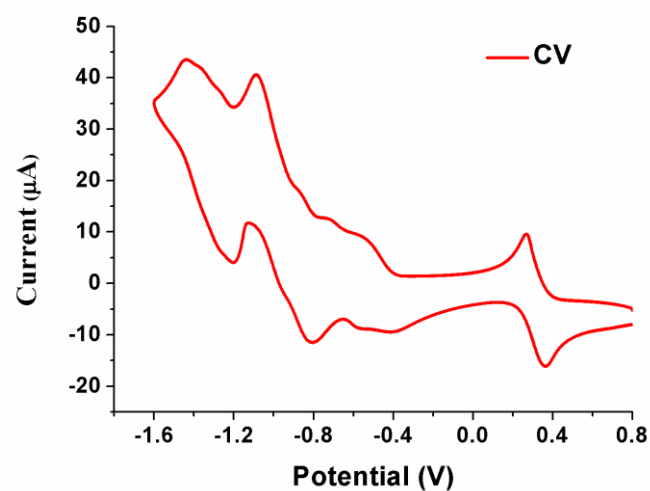


Figure S3. Cyclic voltammogram of **6** and ferrocene as internal standard in CH_2Cl_2 solution at ambient temperature. $c = 5 \times 10^{-4}$ mol/L, $\nu = 100$ mV/s, 0.1 M TBAPF_6 as supporting electrolyte.

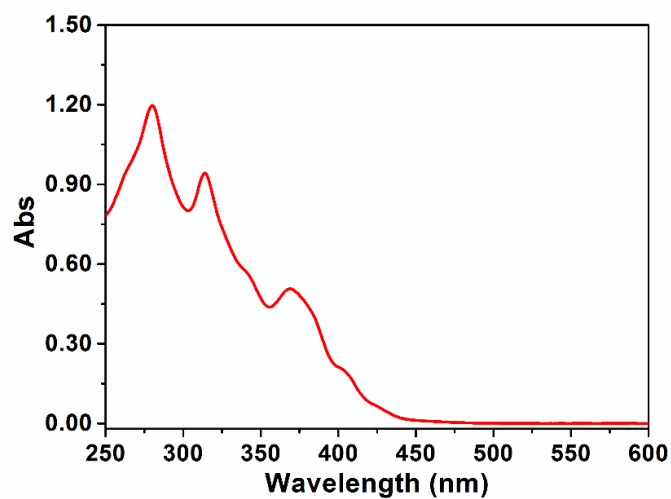


Figure S4. Absorptions of **6** in its neutral state in CH_2Cl_2 solution, $c = 1.0 \times 10^{-5}$ mol/L.

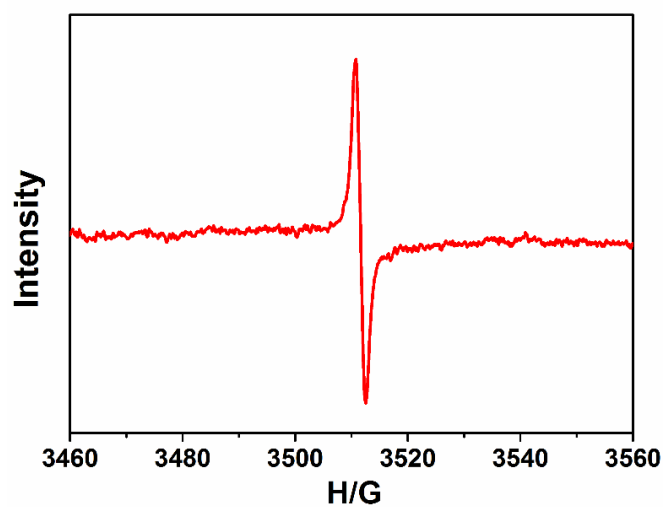


Figure S5. EPR of **6** radical anion in dilute CH_2Cl_2 solution.

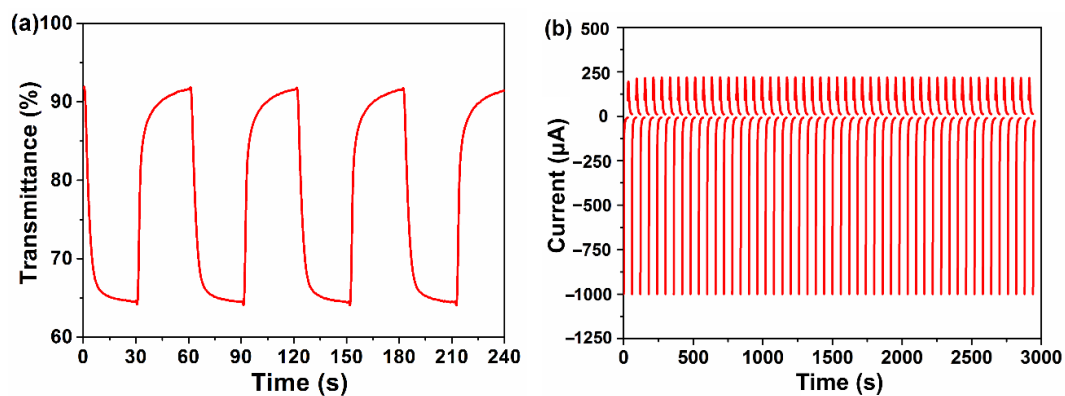


Figure S6. (a) Time response and (b) first 50 cyclic current stability of **6** thin film on ITO glass dipped into CH₃CN/TBAPF₆ (0.1 M) solution between -0.75 and 0.10 V (potentials vs Fc/Fc⁺). The amount of O₂ was estimated to be ~ 739 mg/L and the amount of H₂O was estimated to be ~ 500 mg/L in the commercially-available anhydrous acetonitrile (A.R.).

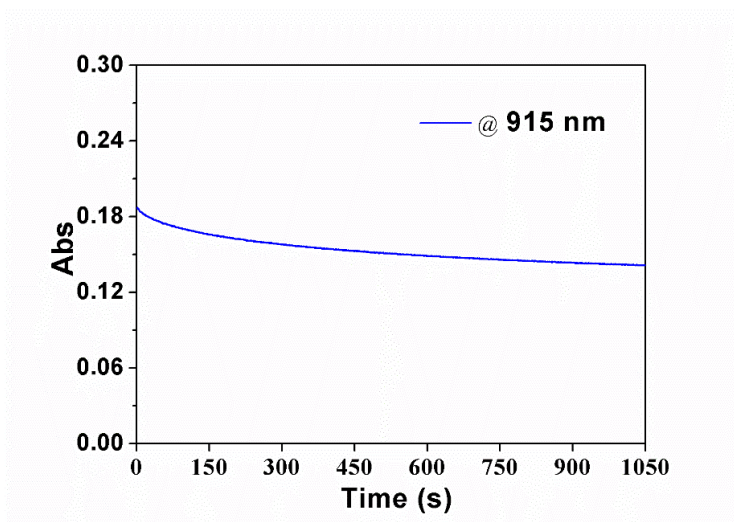


Figure S7. Changes of absorption intensity at 915 nm of the **6** radical anion with time after removal of external voltage

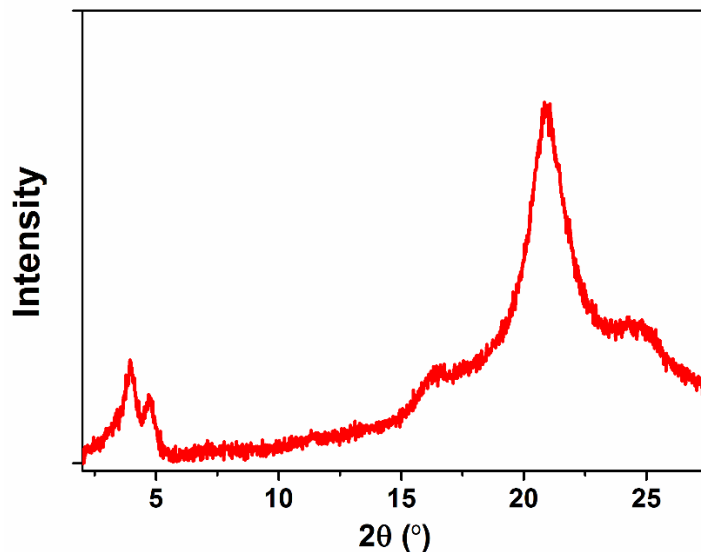


Figure S8. 1D WAXD of **6** thin film at room temperature.

Table S1. 1D WAXD patterns data of **6** thin film at room temperature.

	2θ/degree	d/Å
Peak1	3.942	22.40
Peak2	21.07	4.213

Distances are calculated according to the Bragg's Law: $2d\sin\theta=\lambda$, Where λ is 1.5406 Å.

Formation of Columnar Liquid Crystalline Phase

Further experiments have been carried out to verify its columnar liquid crystalline properties in the solid state instead of the thin film. Thermal behavior of the powder **6** in the solid state were investigated by differential scanning calorimetry (DSC), polarizing optical microscopy (POM), 1-D Wide angle X-ray diffraction (1D WAXD) and 2-D Wide Angle X-ray Diffraction (2-D WAXD).

In the first heating process of DSC, a weak exothermic peak appears at 145 °C (Figure S9. a); meanwhile, a conic texture was observed at 200 °C by POM (Figure S9. b). The conic texture is a typical texture for discotic mesogens in hexagonal columnar crystal phase or rectangular columnar mesophase. Combining with 1-D and 2D WAXD (Figure S9. c and d) curves, we can conclude that liquid crystalline phase has been formed. We can calculate structural parameters of the liquid crystal phase through the following equation:

$$1/d^2 = h^2/a^2 + k^2/b^2$$

Where h , k refer to reciprocal vectors, d is the inter-planar spacing, a and b are lengths in the a axis and the b axis directions of the liquid crystal structure. The calculation results were summarized in Table S2. a and b was calculated from the first two diffraction peaks, and their values match well with the measured one. By further comparing the reciprocal vectors, we can also conclude that it forms rectangular columnar liquid crystal phase in the $p2gg$ symmetry.

At elevated temperature ~ 240 °C, the disappearance of birefringence in the POM test and the disappearance of characteristic diffraction peaks in 1D WAXD curves verify that **6** turns into the isotropic phase. In the cooling process, the isotropic phase system reversibly recovered to the liquid crystal phase. The phase transitions of **6** powders with temperature were demonstrated in Scheme S1.

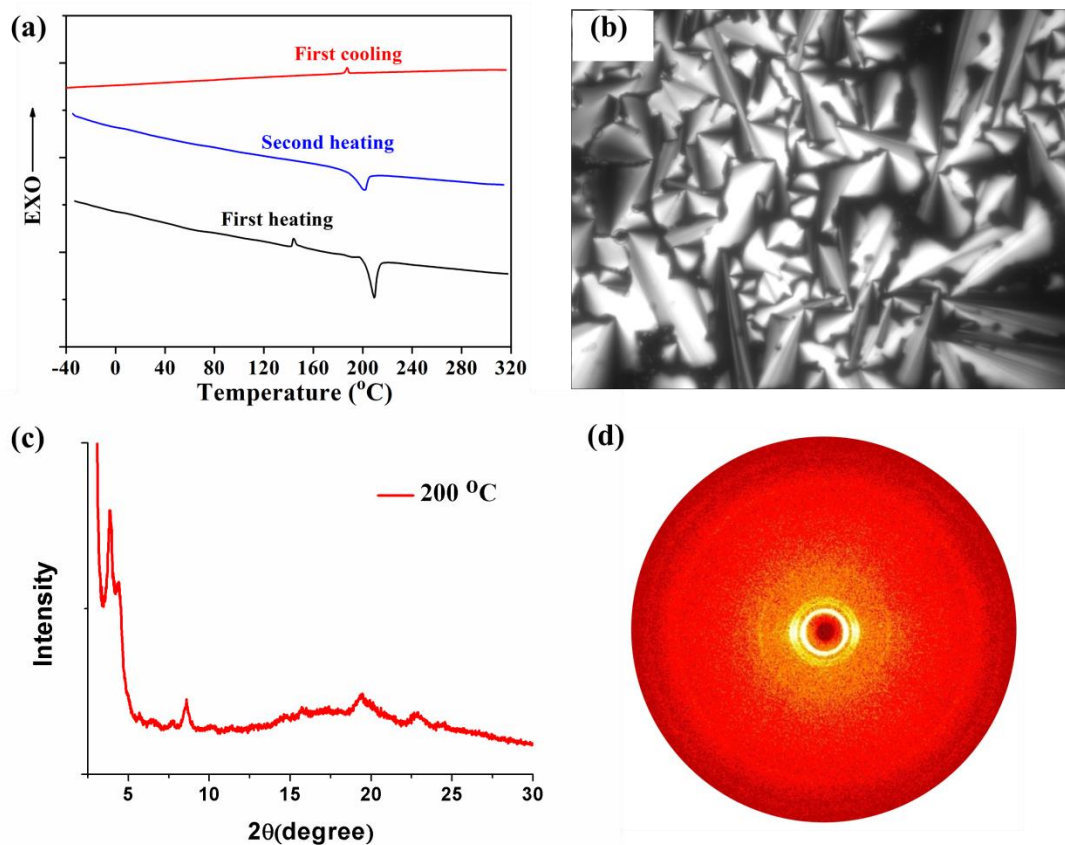
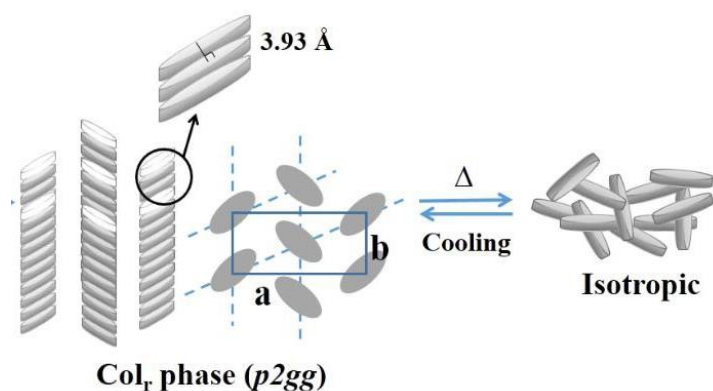


Figure S9. (a) DSC curves for compounds **6** with a heating–cooling scan rate of 10 °C min^{-1} under nitrogen; (b) POM images of **6** at 200 °C upon heating; (c) 1D WAXD of **6** powders at 200 °C; (d) 2-D WAXD image of oriented **6** powders after heating.

Table S2. Structural parameters of **6** measured for each diffraction peak in liquid crystal state.

Entry	hk	$d_{\text{measured}}/\text{Å}$	$d_{\text{calculated}}/\text{Å}$
	20	30.7	30.7
	11	22.9	22.9
$a = 61.4$ Å	31	15.6	15.8
$b = 24.7$ Å	22	11.5	11.5
	32	10.4	10.6

Scheme S1. Phase transitions of **6** in the process of heating and cooling

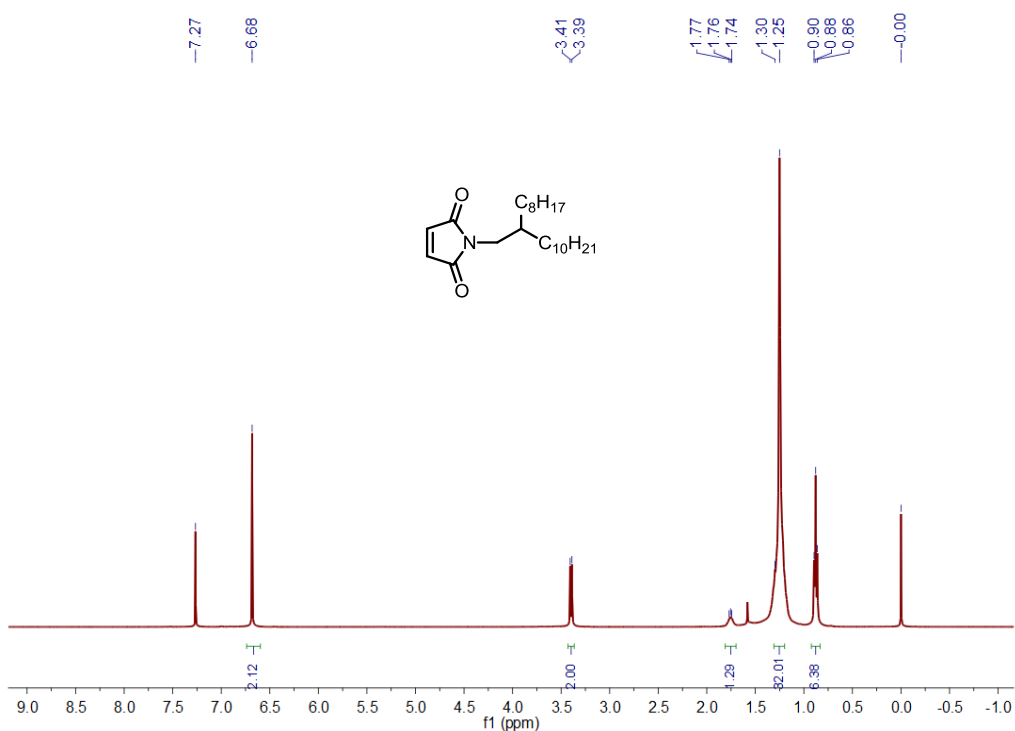


References

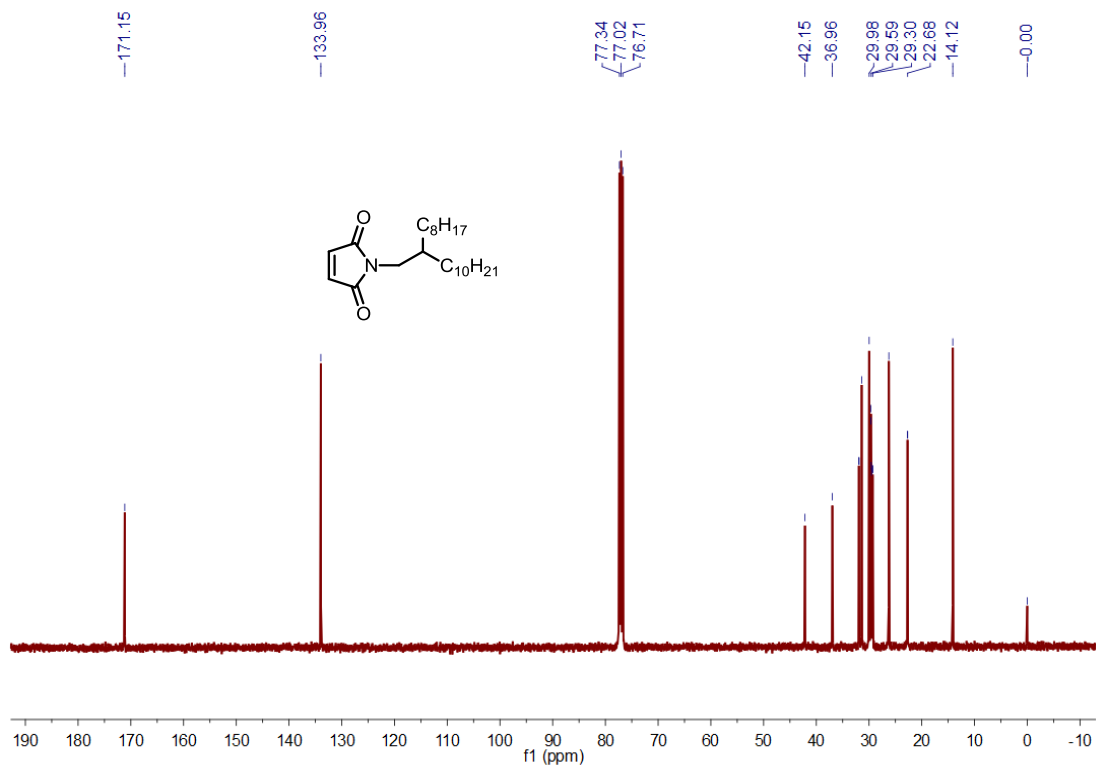
- (1) Frisch, M. J.; Trucks, G. W.; Schlegel, H. B.; Scuseria, G. E.; Robb, M. A.; Cheeseman, J. R.; Scalmani, G.; Barone, V.; Mennucci, B.; Petersson, G. A.; Nakatsuji, H.; Caricato, M.; Li, X.; Hratchian, H. P.; Izmaylov, A. F.; Bloino, J.; Zheng, G.; Sonnenberg, J. L.; M. Hada; Ehara, M.; Toyota, K.; Fukuda, R.; Hasegawa, J.; Ishida, M.; Nakajima, T.; Y. Honda; Kitao, O.; Nakai, H.; Vreven, T.; Montgomery, J. A.; Peralta, J. E.; Ogliaro, F.; Bearpark, M.; Heyd, J. J.; Brothers, E.; Kudin, K. N.; Staroverov, V. N.; Kobayashi, R.; Normand, J.; Raghavachari, K.; Rendell, A.; Burant, J. C.; Iyengar, S. S.; Tomasi, J.; Cossi, M.; Rega, N.; Millam, J. M.; Klene, M.; Knox, J. E.; Cross, J. B.; Bakken, V.; Adamo, C.; Jaramillo, J.; Gomperts, R.; Stratmann, R. E.; Yazyev, O.; Austin, A. J.; Cammi, R.; Pomelli, C.; Ochterski, J. W.; Martin, R. L.; Morokuma, K.; Zakrzewski, V. G.; Voth, G. A.; Salvador, P.; Dannenberg, J. J.; Dapprich, S.; Daniels, A. D.; Farkas, Ö.; Foresman, J. B.; Ortiz, J. V.; Cioslowski, J.; Fox, D. J., *Gaussian09*; Gaussian, Inc.: Wallingford, CT, 2009.
- (2) Dennington, R.; Keith, T.; Millam, J.; *GaussView, Version 3.09*; Semichem, Inc.: Shawnee Mission, KS, 2009.
- (3) Ardecky, R. J.; Kerdesky, F. A. J.; Cava, M. P. *J. Org. Chem.* **1981**, *46*, 1483-1485.
- (4) Hardy, A. D. U.; Macnicol, D. D.; Wilson, D. R. *J. Chem. Soc., Perkin Trans. 2* **1979**, *7*, 1011–1019.

Part 4. ^1H NMR and ^{13}C NMR Spectra

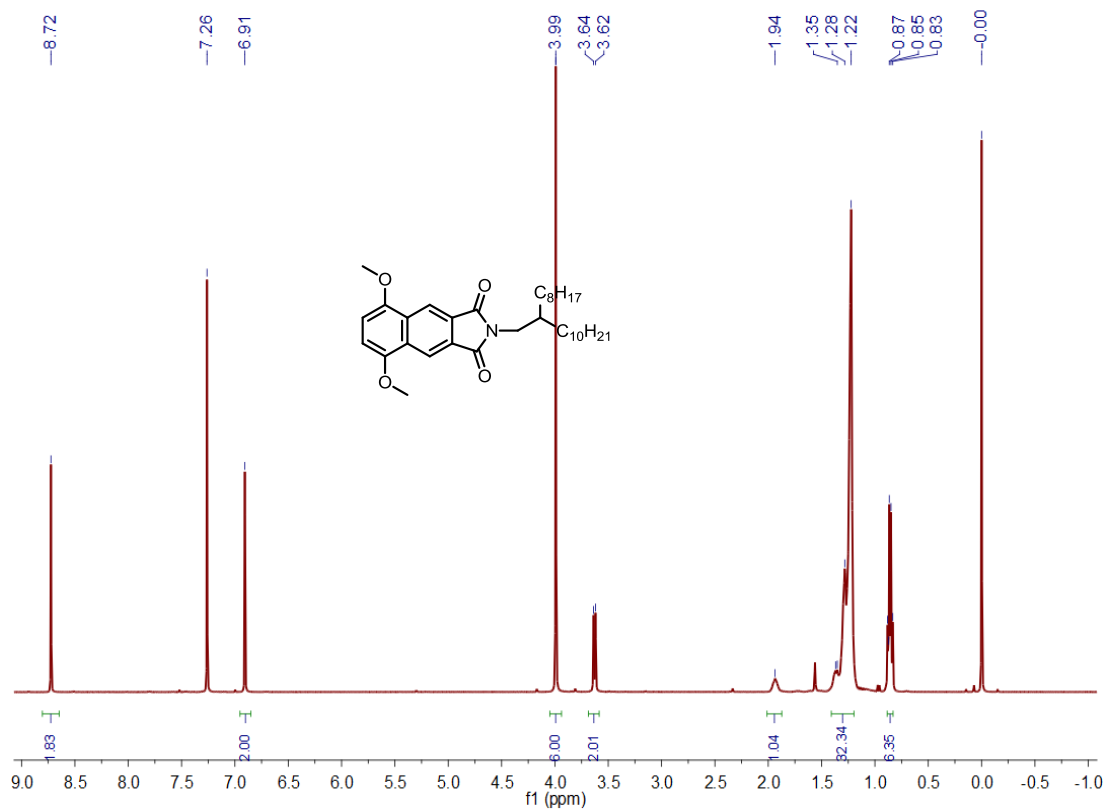
Compound 2, ^1H NMR (400 MHz, CDCl_3)



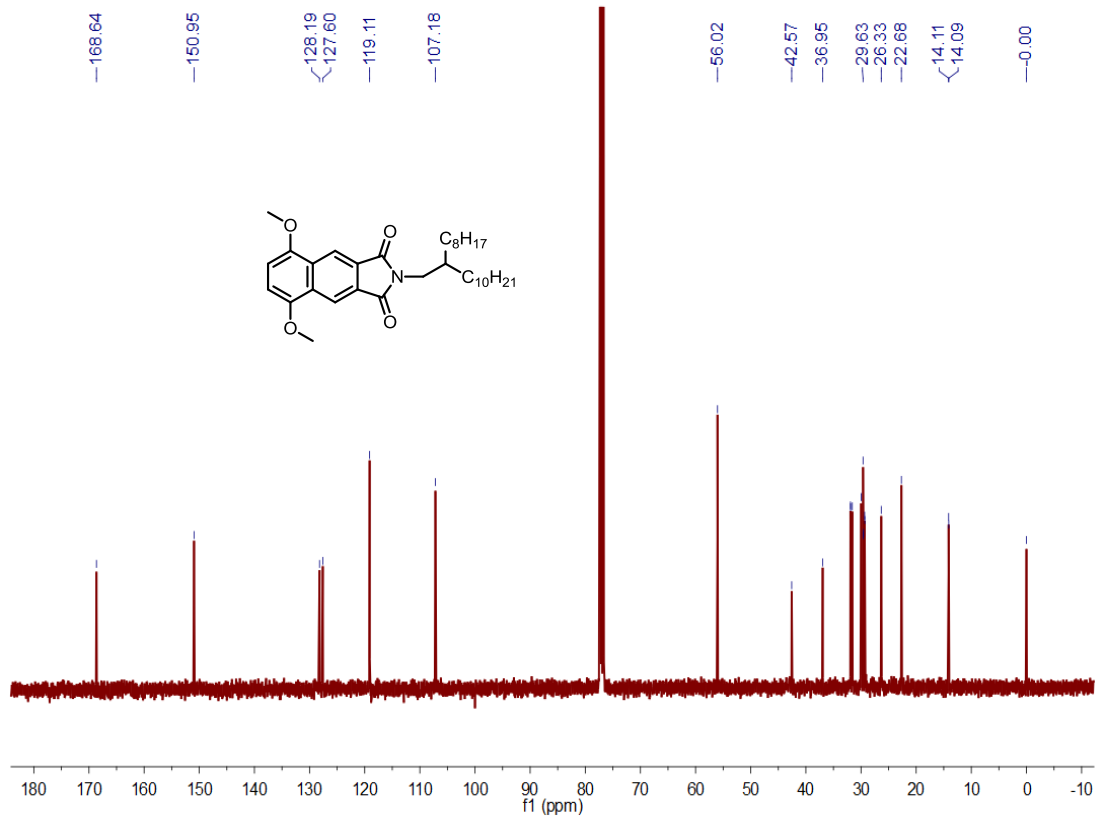
Compound 2, ^{13}C NMR (100 MHz, CDCl_3)



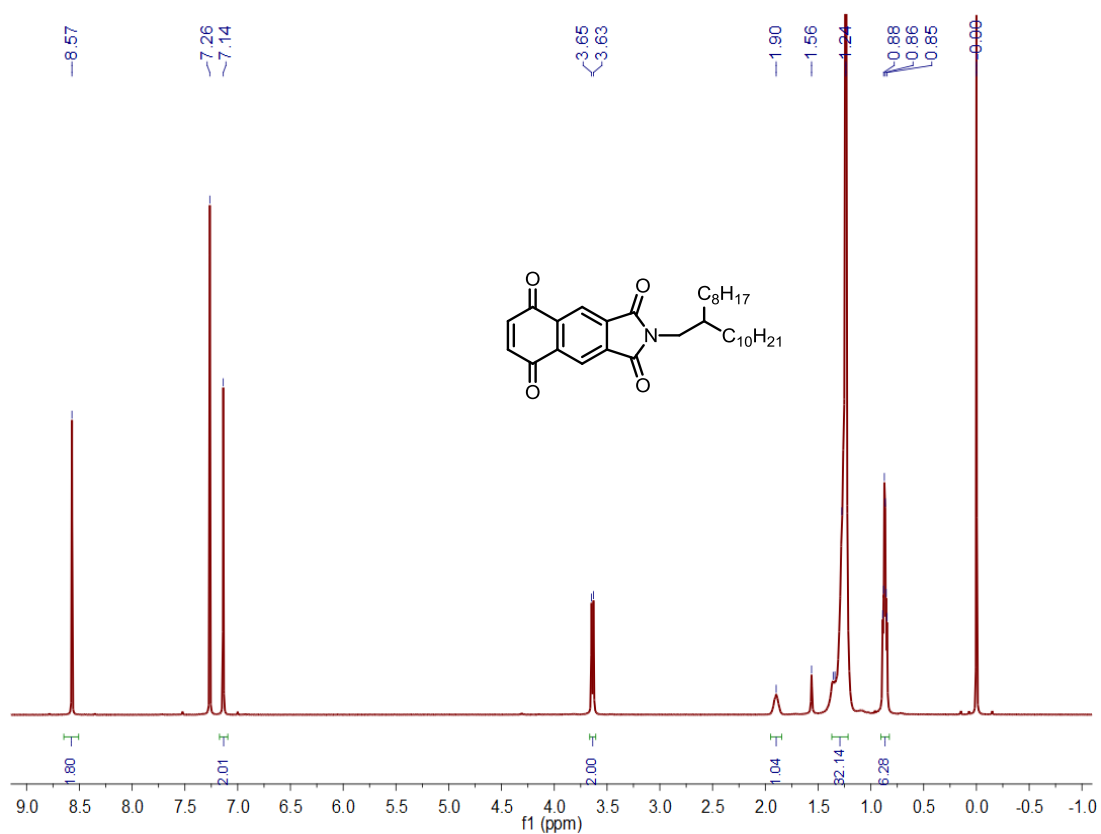
Compound **4**, ^1H NMR (400 MHz, CDCl_3)



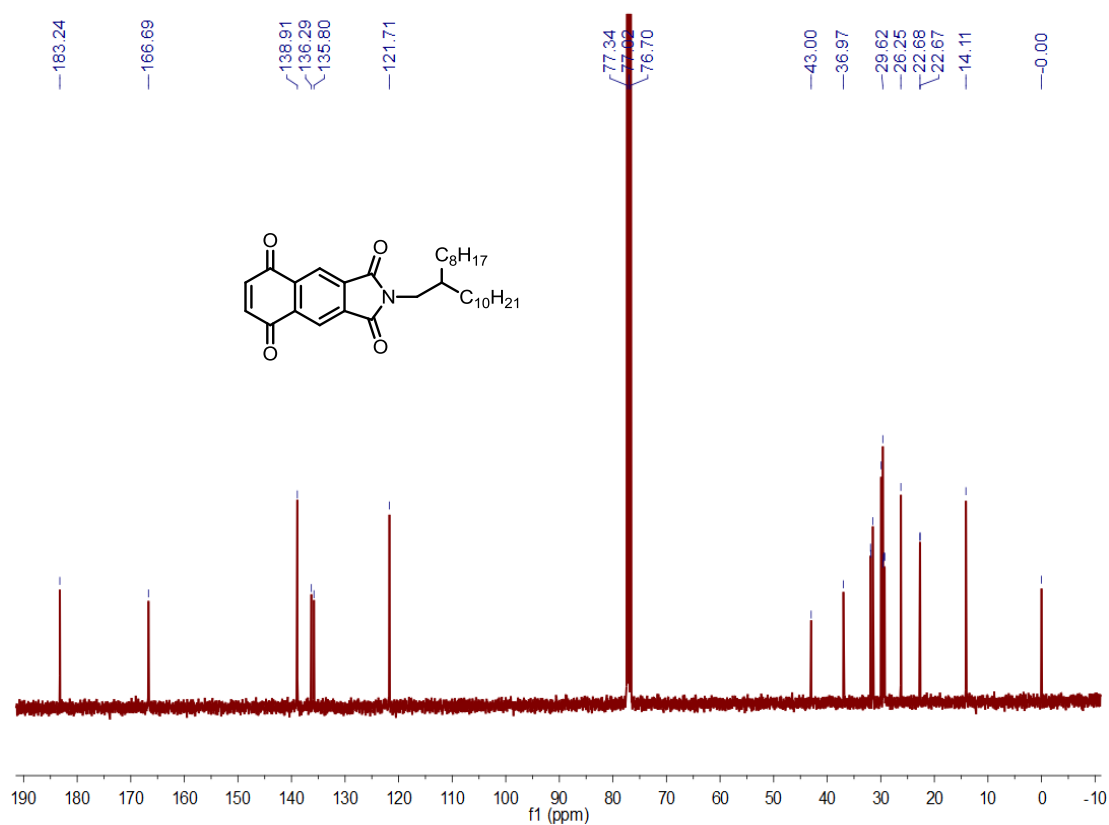
Compound **4**, ^{13}C NMR (100 MHz, CDCl_3)



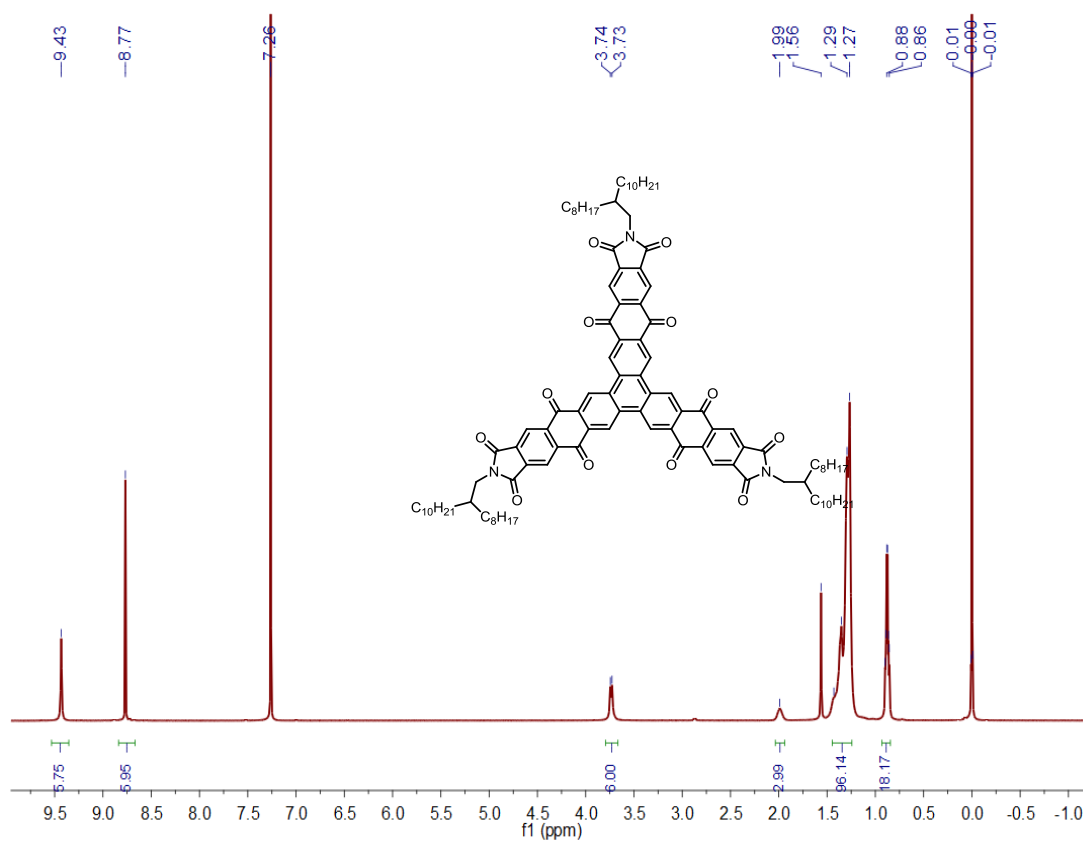
Compound 5, ^1H NMR (400 MHz, CDCl_3)



Compound 5, ^{13}C NMR (100 MHz, CDCl_3)



Compound **6**, ^1H NMR (400 MHz, CDCl_3)



Compound **6**, ^{13}C NMR (100 MHz, CDCl_3)

